

An Efficient Transfer Learning Based Cross Model Classification (TLBCM) Technique for Breast Cancer Prediction using Cyber-Physical System

Sudha Prathyusha Jakkaladiki ^{Corresp., 1}, Filip Maly ¹

¹ Department of Informatics and Quant., University of Hradec Králové, Hradec Kralove, Hradec Kralove, Czech Republic

Corresponding Author: Sudha Prathyusha Jakkaladiki
Email address: sudha.jakkaladiki@uhk.cz

Breast cancer has been the most life-threatening disease in women in the last few decades. The maximum death among women is due to breast cancer because of less awareness and a minimum number of medical facilities to detect the disease in the early stages. In the recent era, the situation has changed with the help of many technological advancements and medical equipment to see breast cancer development. The machine learning technique supports vector machines (SVM), logistic regression, and random forests have been used to analyze the images of cancer cells on different data sets. Although the particular technique has performed better on the smaller data set, accuracy still needs to catch up in most of the data, which needs to be fairer to apply in the real-time medical environment. In the proposed research, state-of-the-art deep learning techniques, such as Transfer Learning, Based Cross Model classification (TLBCM), Convolution Neural Network (CNN) and transfer learning, Residual network (Resnet), and Densenet proposed for efficient prediction of breast cancer with the minimized error rating. The convolution neural network and transfer learning are the most prominent techniques for predicting the main features in the data set. The sensitive data is protected using a Cyber-Physical System (CPS) while using the images virtually over the network. CPS act as a virtual connection between human and networks. While the data is transferred in the network, it must monitor using CPS. The Resnet changes the data on many layers without compromising the minimum error rate. The Densenet conciliates the problem of vanishing gradient issues. The experiment is carried out on the data sets Breast Cancer Wisconsin (Diagnostic) and Breast Cancer Histopathological Dataset (BreakHis). The convolution neural network and the transfer learning have achieved a validation accuracy of 98.3%. The results of these proposed methods show the highest classification rate between the benign and the malignant data. The proposed method improves the efficiency and speed of classification, which is more convenient for discovering breast cancer in earlier stages than the previously proposed methodologies.

1 An Efficient Transfer Learning Based Cross 2 Model Classification (TLBCM) Technique for 3 Breast Cancer Prediction using 4 Cyber-Physical Systems

5 Sudha Prathyusha Jakkaladiki¹ and Filip maly¹

6 ¹Department of Informatics and Quant. methods, University of Hradec kralove , Czech
7 Republic

8 Corresponding author:

9 Sudha Prathyusha Jakkaladiki¹

10 Email address: Sudha.jakkaladiki@uhk.cz

11 ABSTRACT

12 Breast cancer has been the most life-threatening disease in women in the last few decades. The
13 maximum death among women is due to breast cancer because of less awareness and a minimum
14 number of medical facilities to detect the disease in the early stages. In the recent era, the situation
15 has changed with the help of many technological advancements and medical equipment used to detect
16 breast cancer development. The machine learning technique supports vector machines (SVM), logistic
17 regression, and random forests have been used to analyze the images of cancer cells on different data
18 sets. Although the particular technique has performed better on the smaller data set, accuracy still needs
19 to catch up in most of the data, which is not fair enough to apply in the real-time medical environment.
20 In the proposed research, state-of-the-art deep learning techniques, such as Transfer Learning, Based
21 Cross Model classification (TLBCM), Convolution Neural Network (CNN) and transfer learning, Residual
22 network (Resnet), and Densenet proposed for efficient prediction of breast cancer with the minimized
23 error rating. The convolution neural network and transfer learning are the most prominent techniques
24 for predicting the main features in the data set. The sensitive data is protected using a Cyber-Physical
25 System (CPS) while using the images virtually over the network. CPS act as a virtual connection between
26 human and networks. While the data is transferred in the network, it must monitor using CPS. The
27 Resnet changes the data on many layers without compromising the minimum error rate. The Densenet
28 conciliates the problem of vanishing gradient issues. The experiment is carried out on the data sets
29 Breast Cancer Wisconsin (Diagnostic) and Breast Cancer Histopathological Dataset (BreakHis). The
30 convolution neural network and the transfer learning have achieved a validation accuracy of 98.3

31 INTRODUCTION

32 In the modern world, although there are much medical equipment and advancements in medicine, nearly
33 two million women are affected by the cruelest disease, breast cancer. Cancer occurs in the human body
34 when there is a cell growth called mutations. Few prominent techniques and methods are available to
35 predict breast cancer in its early stages in middle-aged women. Mutation divides the cell and grows
36 unconditionally in a chaotic way. Moreover, the progress of this mutation will be abnormal. Consequently,
37 it ends up in the formation of tumor cells in the human body. Breast cancer occurs particularly in a
38 female body when there is a malignant called a cancerous cell. As it grows continuously, it may spread
39 to other parts of the human body and could automatically result in death. Early detection of the disease
40 will help the women to survive and decrease the death rate. The classification of mammogram images to
41 detect breast cancer is based on techniques such as fuzzy systems, machine learning, and deep learning.
42 Image processing converts the data obtained from medical devices such as mammograms. Also, they are
43 converted into a digital form of processing. During the conversion of images to digital format, useful
44 information will be extracted from the images for analyzing the data. Specifically, the pixels are the

45 information about a particular value in a precise location. The image processing is performed in the
46 following steps.

- 47 1. The image is obtained from medical devices such as optical scanners or X-rays.
- 48 2. Enhancement of the images, including data compression to extract the features.
- 49 3. The result will be obtained by analyzing the quality and the classification.

50 Classification of mammogram images is done by using supervised or unsupervised machine learning
51 algorithms. These algorithms are based on the shape of the cancer cell, which is gentle, malignant, or
52 abnormal.

53 The computer-aided design detection (CAD) on mammogram images is used to detect the occurrence
54 of breast cancer (33; 25). Although the performance of the techniques is better, it has many disadvantages.
55 Specifically, handcrafted feature extraction is the most tedious process. Compared to the other machine
56 learning technologies, the traditional method involves a lot of handcrafted features. It is very difficult and
57 has no generalized procedure. The solution for the existing traditional handcraft-based feature extraction
58 is the convolutional neural network. (23; 14).

59 According to previous research, the convolutional neural network performs better than the traditional
60 method for getting features from the images. The classic convolutional neural network alexnet has won
61 the challenge in imagenet, where it contains 1000 classes of colored images, and it has got 83.6

62 In this proposed research work, the cross-modal deep learning approach is used to predict breast
63 cancer from mammographic images. Preprocessing of images and classification is a part of the model.
64 The images are preprocessed for enhancement and extraction of important information from the images.
65 The image is resized for clarity so as to fit into the model. The model includes Convolutional Neural
66 Network (CNN), transfer learning, Resnet, and Densenet.

67 The key contribution of our research work is as follows:

- 68 1. The features are extracted using the convolution neural network along with the transfer learning
69 technique.
- 70 2. The weight and biases of the pre-trained model are fine-tuned automatically to analyze the features
71 of the Mammogram images
- 72 3. The Resnet and Densenet models are employed to compare the accuracy
- 73 4. The learning rate change and data augmentation apply to avoid the over-fitting of the model.

74 The remaining parts of the paper are arranged in the following order. In section 2, the literature
75 reviews on convolutional neural network transfer learning and augmentation on the mammographic image
76 dataset are analyzed. In section 3, the dataset and the experimental setup are discussed. In section 4, the
77 results of the proposed model are discussed. In section 5, the conclusion is given.

78 RELATED WORK

79 Deep learning is a concept that has been established to effectively extract the pertinent information from
80 the raw images and use it for the classification process in order to overcome the limitations of classic
81 machine learning approaches. (19),(3).

82 The convolutional neural network can be applied in three major ways; 1. pre-trained model of CNN.
83 2. training the CNN from the scratch. 3. fine-tuning of CNN (12; 24), has shown numerous machine
84 learning algorithms that are employed for detecting breast cancer on mammographic images. In the study,
85 the databases that are most commonly used are Digital Database for Screening Mammography (DDSM)
86 and MIAS, as proposed by (PUB et al.). M. Heath et al. used a 10-fold cross-validation technique to test
87 the model on the database. S. Khan (17), Y.-D. Zhang (39) used the automatic feature extraction method
88 with CPS instead of the handcraft feature extraction technique such as fractional Fourier transform and
89 Gabor filter along with the classifiers such as Support Vector Machine (SVM).

90 (10) has proposed many neural networks and example methods for the classification of breast cancer.
91 (29) had focused on convolutional neural networks. It produced excellent results when compared to the

92 other neural networks in terms of feature extraction and classification in mammogram images. (13)
93 had proved in his study that the convolutional neural network was superior to the other traditional
94 machine learning techniques for extracting the features along with transfer learning using CPS. Deep
95 learning techniques are implemented in the medical field for obtaining better outcomes, along with tough
96 challenges in the input data compared to the other fields. Transfer learning is used by different physicians
97 and technicians for analyzing various medical images, which gives better results in diagnosis (34; 22)].

98 (13), had achieved 88 (1; 26) enhanced the study accuracy of breast cancer by utilizing the method of
99 Double Shot Transfer Learning (DSTL) with the help of pre-trained networks. Unlike the other models
100 which use the smallest medical data, the proposed model employs a larger data set as a target data set
101 for fine-tuning. The weight and the bias are fine-tuned from the pre-trained model. The fine-tuning of
102 parameters is achieved with the help of the target dataset.

103 An approach for Deep Learning (DL) has been proposed by Dongdong Sun et al. dubbed D-SVM
104 for human breast cancer prediction prognosis. The program has successfully discovered hierarchy and
105 created an abstract representation from raw input data combined approach of traditional classification
106 (37). In order to identify the architectural distortion from digital mammography, (30) have examined
107 various deep-learning techniques. The primary objective of their research was to find the abnormalities
108 that are the signs of advanced diseases like masses and micro-calcification. Only 12

109 (31) proposed a transfer learning approach with the help of three kinds of networks; 1. VGG-f, 2.
110 Caffe, and 3. VGG-m. The output was tested in two cases while fine-tuning the model. In the first case,
111 image normalization was applied to find the abnormal letters in mammogram images. In the second case,
112 the model of no image normalization was applied for testing. In the proposed model, both support vector
113 machines and convolution neural networks are employed. Features are extracted using the convolution
114 neural network, and the classification is handled by the support vector machine. The extracted features
115 by the convolution neural network are passed to the support vector machine for the classification of
116 mammogram images for identifying the possibilities of breast cancer.

117 It is aimed to develop an end-to-end deep learning framework for multi-label breast lesion detec-
118 tion, which is motivated by the success of Convolutional Neural Networks (CNNs) in single-label
119 mammography classification (15),(2),(21). In order to create an autonomous multi-labeling framework
120 that can aid the radiologist in providing his patients with a thorough report and more accurate diag-
121 noses, we aim to make use of the highly expressive convolutional neural network architecture (CNN)
122 (20),(27),(9),(38),(35). Numerous microwave imaging techniques, including microwave tomography and
123 radar-based imaging, were researched. Some imaging diagnostic techniques were described by Lu et al.
124 [42-46] for the diagnosis of breast cancer. It looked into how computer vision and machine learning could
125 detect breast cancer. On the basis of mammographic images, the effectiveness of various approaches was
126 examined.

127 (16) proposed a new feature extraction technique, Speed-Up Robust Features (SURFs), which is
128 k-means convergence on a mini dataset. An additional layer is introduced in the classification process.
129 70% of the data from the dataset is used for training and 30% of the data is used for testing models.
130 Classification support vector machines and deep neural networks are employed. The result got from this
131 model is sure that this deep neural network performs better than the decision tree model. The accuracy is
132 improved by employing the convolution neural network model on many datasets, which is equal to 87.5%.

133 Deep learning techniques built on Convolution Neuronal Networks (CNN) have recently seen con-
134 siderable success in the field of biomedical image analysis. Examples include the recognition of mitotic
135 cells in microscopic pictures (28), the detection of tumors (6), the segmentation of neural membranes
136 (7), the detection and classification of immune cells (5), and the quantification of mass in mammograms
137 (11),(4),(8).

138 PROPOSED TLBCM ARCHITECTURE

139 The best cancer detection method is shown in figure 1. The deep learning approaches convolution neural
140 networks (CNN), Resnet, and Densenet are used to extract the salient features from the mammogram
141 image dataset. The dataset is processed to identify and classify the images based on benign and malignant.

142 Preprocessing

143 In this section, the pre-processing of data is described. Data augmentation is applied to the data set to
144 increase the number of data to avoid over-fitting during training and testing of the model. The main

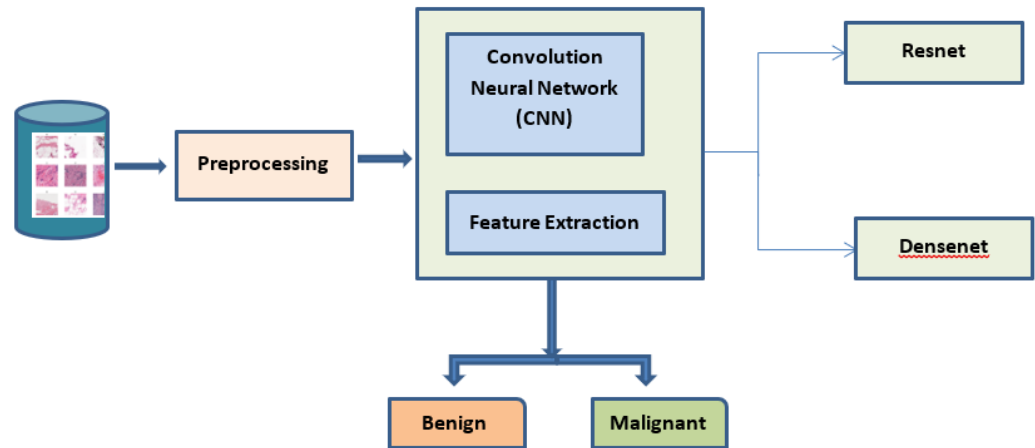


Figure 1. Proposed System

145 issue with the medical dataset is the minimum number of samples. This dataset can be enlarged with the
 146 help of data augmentation and scaling. The missing data cells are replaced with zero. The benign and
 147 the malignant data are balanced by introducing a random noise in the data. The 241 malignant data are
 148 doubled as 482. This is achieved by the array of random numbers. The standard deviation sigma value is
 149 0.1. The feature values are scaled using the formula

$$\frac{v_f - v_{min}}{v_{max} - v_{min}} \quad (1)$$

150 v_f is the feature value. v_{min} is the minimum value, v_{max} is the maximum value

151 The square root transformation is applied to the resultant dataset.

152 Convolution Neural Network with transfer learning

153 Transfer learning is the concept of taking the already learned features from other works to apply to the
 154 current problem without the need to start from the beginning. Normally, transfer learning is built on the
 155 convolution neural network (CNN) on a well-known dataset. The convolution neural network reduces
 156 the input and analyzes the features to differentiate it from the other images. It contains several layers
 157 that include a convolution layer, max pooling layer, fully connected layer, and batch normalization. The
 158 convolution layer in the CNN extracts the features from the given input mammogram images. In this
 159 layer, the images are convolved with a kernel or filter. The kernel is multiplied by the match patch. The
 160 filter size is matched with the input size and width, and height of the filter according to the network
 161 deployment. After the convolution, the input is transformed through subsampling, which can be max
 162 pooling, min pooling, or average pooling. The pooling filter is chosen as an odd number. It is responsible
 163 for dimensionality reduction, which results in minimizing the overfitting issues. The max-pooling layer in
 164 the model is used to minimize the sample in the proposed model. This is used to reduce the complexity of
 165 the model when the data is transferred from one layer to another layer. It is used to initiate invariance.
 166 Fully connected players are on the top of the model that is connected to each other.

In the proposed method, Resnet 50 is used, which is inherited from the base model Resnet. Figure 2 shows the architecture of Resnet 50. It comprises nearly 50 layers with the residual block. Further, it reduces the computation process and the complexity of the model. Resnet 50 comprises convolution layers, normalization layers, and residual blocks. There are 16 residual block modules in between the pooling layers. The filter size used here is 3×3 . This pointer is used to perform the spatial convolution operation for the classification of benign and malignant images in the dataset. The input value x is mapped to the features of output $O(x)$.

$$O(x) = F(x) + x \quad (2)$$

The error from the output is $F(x)$. If the value of $F(x)$ is 0, then the output feature is exactly the same as the target output. Otherwise, it deviates from the target and the weight needs to be adjusted in the

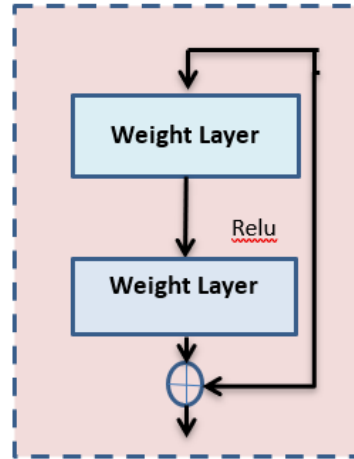


Figure 2. Resnet Architecture

Table 1. CNN training architecture integrated with Transfer learning

| Layer | Particulars |
|-----------------------|----------------------------------|
| Input | RGB image |
| Convolution layer 1 | Conv_3-32 + ReLU |
| Max pooling Layer 1 | MaxPool_2 |
| Convolution layer 2 | Conv_3-32 + ReLU |
| Max pooling Layer 2 | MaxPool_2 |
| Convolution layer 3 | Conv_3-64+ ReLU |
| Max pooling Layer 3 | MaxPool_2 |
| Fully Connected Layer | FC_64 + ReLU(with Dropout = 0.5) |
| Output | (Softmax) |

hidden layers.

$$y = F(x, \{V_j\}) + V_j x \quad (3)$$

¹⁶⁷ V_j is the parameter value which implies the weight to be adjusted in the input shape.

Densenet is the inherited idea of Resnet. The Densenet does not contain any constraints for the number of convolution layers and the width of the layers. The parameters are reduced in the Densenet; hence it avoids redundant features with the help of the feature-reused method. Densenet is used to avoid the vanishing gradient problem. The dense net concatenates the feature map from the different layers to reuse the learned features from the previous layers. Let D_i is the output of the i^{th} layer.

$$D_i = H(D_{i-1}) \quad (4)$$

Then the dense connection of the layers is termed as,

$$D_i = H(D_0, D_1, D_2, \dots, D_{i-1}) \quad (5)$$

¹⁶⁸ The entire architecture of TLBCM architecture is shown in figure 3 The transfer learning is done with
¹⁶⁹ the help of Resnet 50 architecture, which is used as the pre-trained model to reduce the time complexity
¹⁷⁰ and space complexity. Densenet uses the features extracted from the previous layer for the training. The
¹⁷¹ dropout value of the model is 0.5.

¹⁷² Table 1 Shows the CNN architecture, which is integrated with the pre-trained model. The convolution
¹⁷³ layer and the fully connected layers are associated with the activation function (Rectified Linear Unit)
¹⁷⁴ ReLU. The output layer is associated with the Softmax activation function, which is used to distinguish
¹⁷⁵ the malignant and benign data.

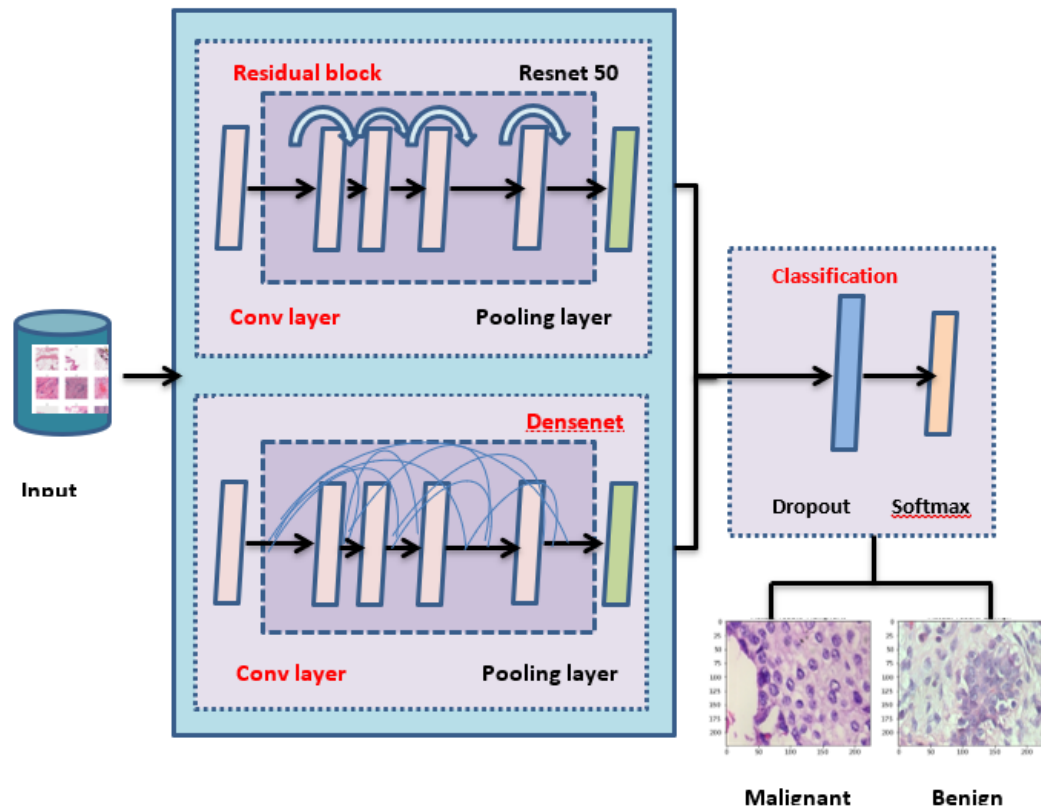


Figure 3. TLBCM architecture

EXPERIMENTAL SETUP

176

177 The experiment is carried out on the Python 3.6 environment, Keras as a framework and Tensor Flow
 178 as a backend. Two datasets are employed for the proposed research work; Breast Cancer Wisconsin
 179 (Diagnostic) and Breast Cancer Histopathological Database (BreakHis).

Dataset

180

181 The experiment is carried out on the Breast Cancer Wisconsin (Diagnostic) Data Set, a multivariate dataset
 182 that comprises 569 instances with 32 attributes. The dataset comprises 357 malignant and 212 benign data.
 183 Figure 4 Shows the data distribution of the Wisconsin database. The dataset comprises 357 malignant and
 184 212 benign data.

185

Figure 5 shows the dataset features' mean value. The mean values are calculated in terms of benign
 186 and malignant. It shows the linear pattern between the area, perimeter, and radius.

187

The dataset comprises ten real-valued features for each cell nucleus. Table 2 Shows the real-valued
 188 features and their mean values for sample data. It includes radius, texture, area, perimeter, compactness,
 189 smoothness, concave points, concavity, fractal dimensions, and symmetry.

190

Figure 6 shows the sample of benign and malignant cell structures. The malignant cancer cells are the
 191 breast tumors and the benign cell structures are the non-cancer and normal cell structures. The benign are
 192 the lumps that are not identified as cancer cells.

193

Another dataset used in the proposed paper is Breast Cancer Histopathological Database (BreakHis).
 194 The dataset comprises microscopic images from 82 different people. Table 3 shows the dataset counts
 195 based on the magnification. The magnifying factors are 40X, 100X, 200X, and 400X. The total number
 196 of benign in the dataset is 2480. The total number of malignant data is 5429.

197

The figure 7 shows the data distribution. A large number of data is identified in the 100X magnification.
 198 The number of data is 1437. The least data identified in the magnification is 400X. The number of data in
 199 this field is 1232.

200

Figure 6 (36) shows the different magnification samples of malignant cancer. The magnificent factor

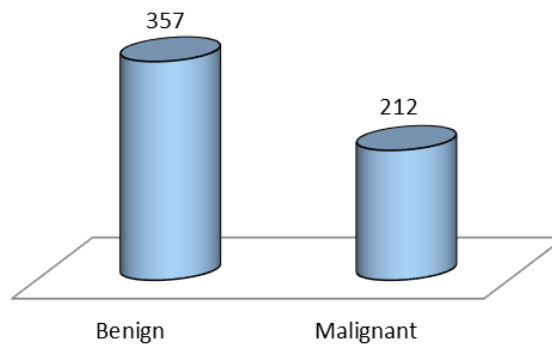


Figure 4. Wisconsin [Diagnostic] data distribution

Table 2. Feature names of sample data

| Parameter | Mean Value of Sample 1 | Mean Value of Sample 2 |
|-------------------------|------------------------|------------------------|
| mean radius | 17.99 | 20.57 |
| mean texture | 10.38 | 17.77 |
| mean perimeter | 122.8 | 132.9 |
| mean area | 1001 | 1326 |
| mean smoothness | 0.1184 | 0.08474 |
| mean compactness | 0.2776 | 0.07864 |
| mean concavity | 0.3001 | 0.0869 |
| mean concave points | 0.1471 | 0.07017 |
| mean symmetry | 0.2419 | 0.1812 |
| mean fractal dimension | 0.07871 | 0.05667 |
| worst texture | 17.33 | 23.41 |
| worst perimeter | 184.6 | 158.8 |
| worst area | 2019 | 1956 |
| worst smoothness | 0.1622 | 0.1238 |
| worst compactness | 0.6656 | 0.1866 |
| worst concavity | 0.7119 | 0.2416 |
| worst concave points | 0.2654 | 0.186 |
| worst symmetry | 0.4601 | 0.275 |
| worst fractal dimension | 0.1189 | 0.08902 |

| Magnification | Benign | Malignant | Total |
|-----------------|--------|-----------|-------|
| 40X | 652 | 1,370 | 1,995 |
| 100X | 644 | 1,437 | 2,081 |
| 200X | 623 | 1,390 | 2,013 |
| 400X | 588 | 1,232 | 1,820 |
| Total of Images | 2,480 | 5,429 | 7,909 |

Table 3. Breast Cancer Histopathological Database (BreakHis) dataset counts based on magnification

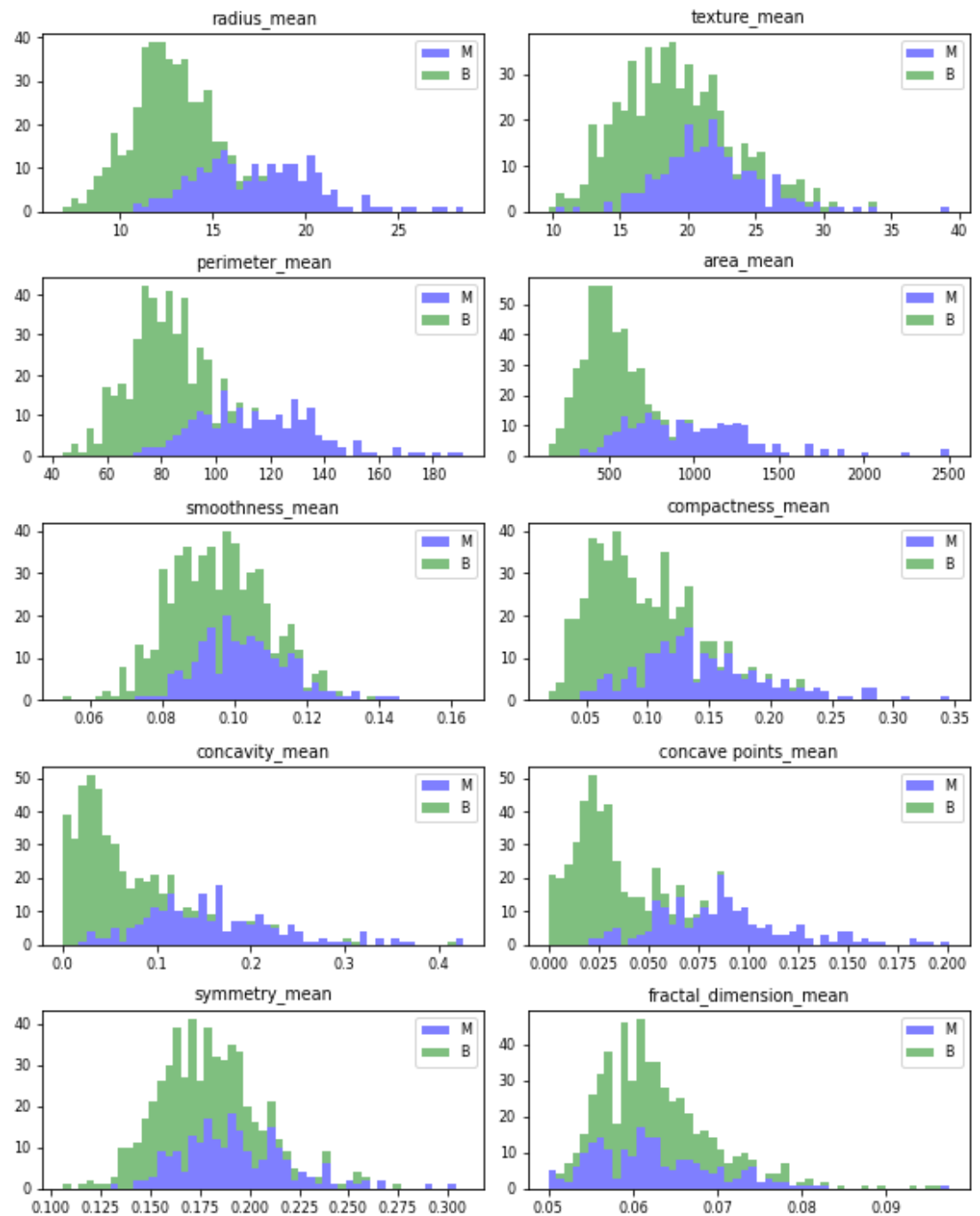


Figure 5. Mean values of Wisconsin's real-valued features

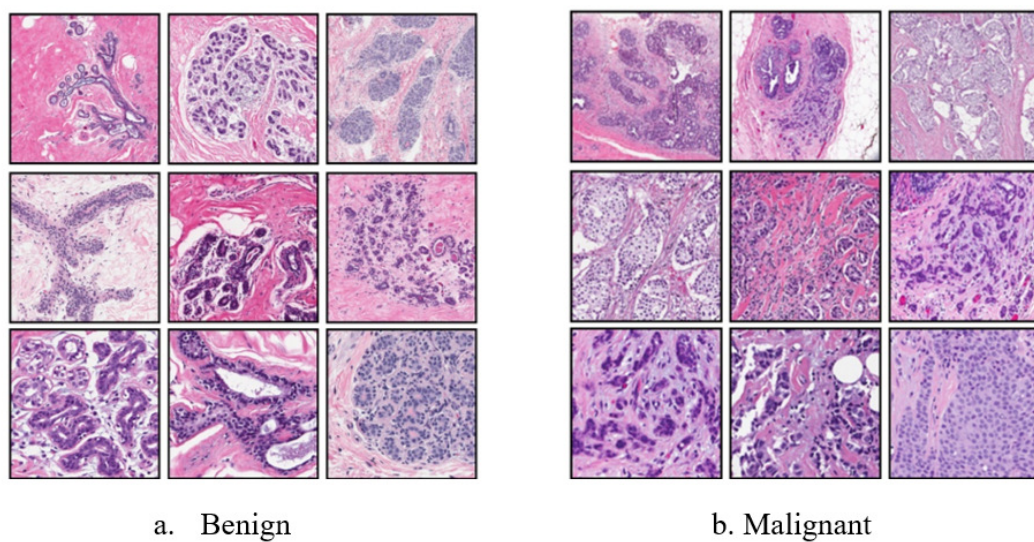


Figure 6. Benign and malignant data sample

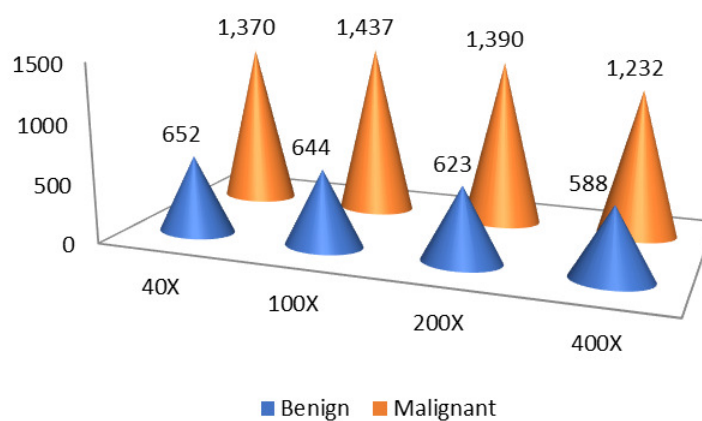


Figure 7. BreakHis data distribution

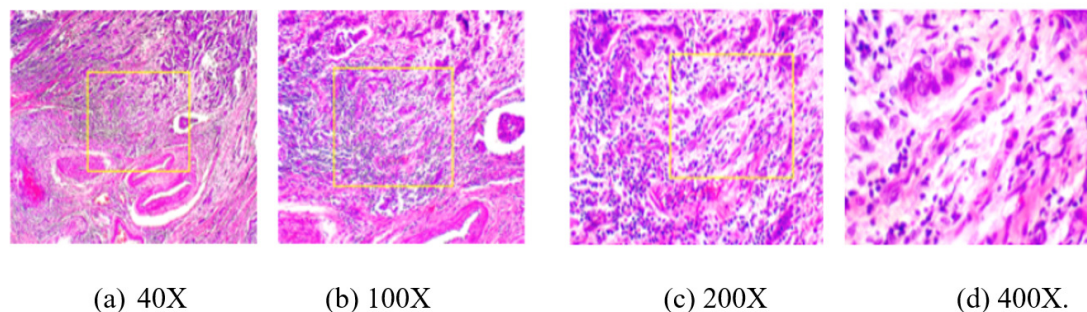


Figure 8. Different Magnification of Malignant Cancer

Table 4. TLBCM model construction Model: Sequential₁

| Layer (type) | Output Shape | Param # |
|-------------------------------|--------------------|----------|
| densenet201 (Model) | (None, 7, 7, 1920) | 18321984 |
| obal_average_pooling2d_1 | (None, 1920) | 0 |
| dropout_1 (Dropout) | (None, 1920) | 0 |
| batch_normalization_1 (Batch) | 0 | 0 |
| (None, 1920) | 7680 | 0 |
| dense_1 (Dense) | (None, 2) | 3842 |

201 400X shows the clear and magnified view of cancer. The enormous size of tissue is removed from the
 202 patient under the anesthetic and the tissue is analyzed to capture this magnified view of the cancer cells.
 203 The benign cells are always relatively slowed-growing and unharmed. Malignant cancer is fast-growing
 204 and has the possibility of spreading to the nearest cells and tissues.

205 Total params: 18,333,506

206 Trainable params: 18,100,610

207 Non-trainable params: 232,896

208 Table 4 shows the parameter values from the model construction for the Densenet. The total parameters
 209 from the input are 18,333,506, and the trainable parameter for the model is 18,100,610.

210 Hyperparameter Tuning

211 Adam is the most widely used optimizer for the medical-related data set to train and test. Compared to
 212 SGD, Adam produces good accuracy in recognizing the output. When the data set comprises a minimum
 213 number of medical data, over-fitting will be a severe issue during model testing and training. The initial
 214 learning rate is taken as 0.0001. For the upcoming epoch, the learning rate is reduced to 0.1 to improve
 215 the accuracy of the recognition. The model is trained for the 20 epochs. The dropout layer is added to the
 216 model to inactivate some neurons during the training process. The dropout layer is added to the Resnet,
 217 and then the Densenet model is with a rate of 0.2. For the fully connected layer, the dropout value is 0.5.

218 RESULT AND DISCUSSION

219 In this experimental setup, 80

220 Figure 7 (18) shows the sample predicted and actual results.

221 The model's performance is assessed using the accuracy recall, precision, F1 score, and accuracy,
 222 which are the vital data collection and measurement factors. Both precision and accuracy predict the
 223 measurement against the actual output. Accuracy is the measurement of the expected value, and precision
 224 measures the reproducible value even if it deviates from the target output.

$$Accuracy = \frac{\text{Total number of correct prediction}}{\text{total number of prediction}} \quad (6)$$

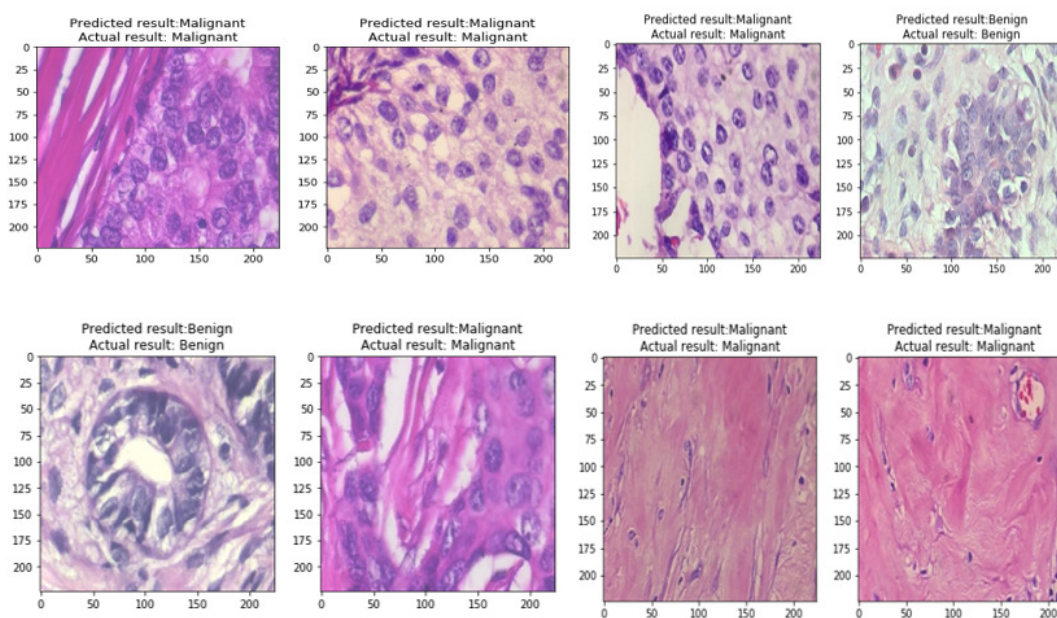


Figure 9. Predicted vs. Actual result

$$\text{Precision} = \frac{\text{True positive}}{\text{All positive}} \quad (7)$$

225 The measurement of True positive recalls and the F1 score is the mean value of precision and recall.

$$\text{F1 Score} = \frac{2 * (\text{Recall} * \text{Precision})}{(\text{Recall} + \text{Precision})} \quad (8)$$

Where ,

$$\text{Recall} = \frac{\text{correctly predicted positive value}}{\text{Total positive value}} \quad (9)$$

Figure 10 Shows the Receiver Operating Characteristic curve (ROC) to measure the performance of the proposed classification. The final area under the ROC curve (AUC) is predicted as 0.692. Moreover, the proposed model has a positive and a negative rate. The true positive rate is calculated using the formula.

$$T_r = \frac{T_p}{T_p + F_n} \quad (10)$$

The false positive rate is calculated as:

$$F_r = \frac{F_p}{F_p + T_n} \quad (11)$$

226 T_p is True Positive and T_n is True negative. F_p is False Positive and F_n is False negative. The AUC Is
227 the aggregate measurement of the performance across the all epoch.

228 Model Evaluation

229 Figure ?? The confusion matrix is used to analyze the performance of the proposed model. It is a two ×
230 two matrix that indicates the target classes. There are two target classes, namely benign and malignant.
231 The predicted values are represented as columns, and the target classes are defined as rows. From the
232 confusion matrix, it is observed that only a few data samples are misclassified as malignant instead of

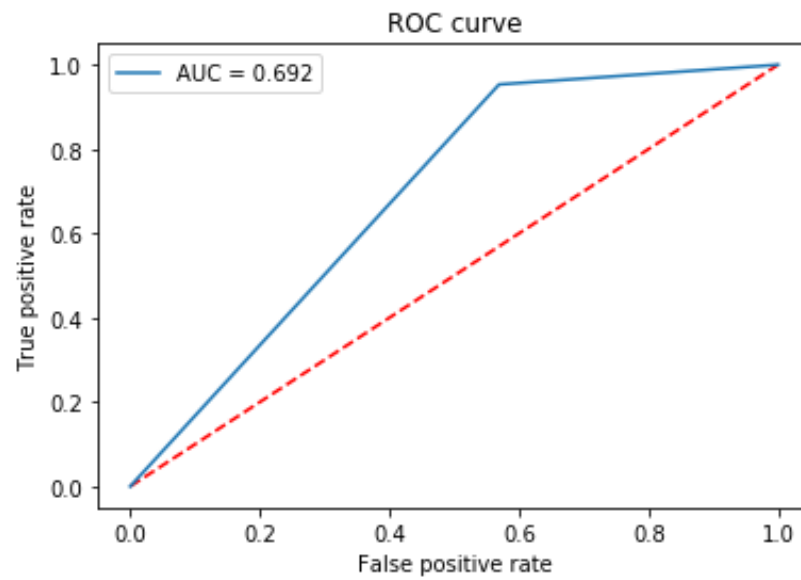


Figure 10. ROC curve

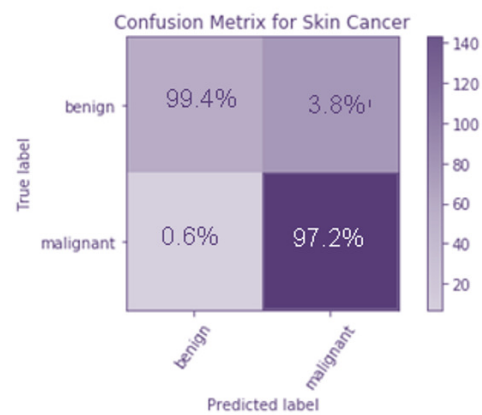


Figure 11. Confusion matrix of TLBCM model

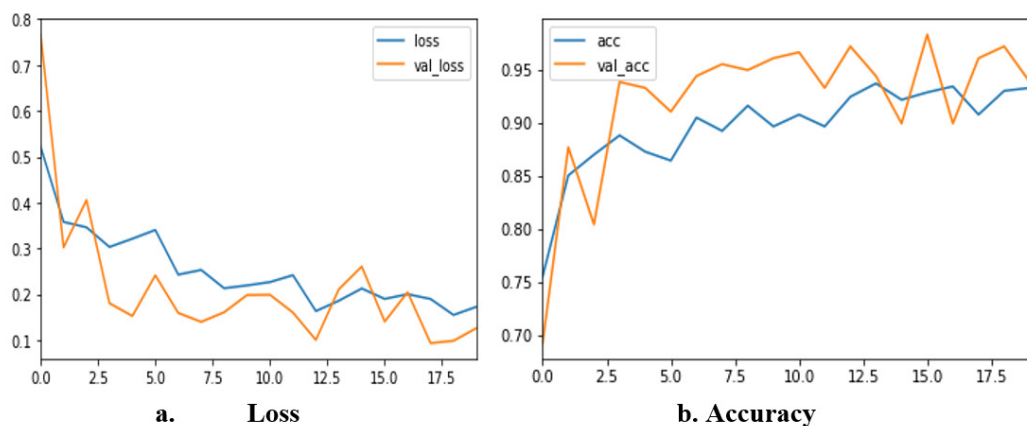


Figure 12. Accuracy and Loss of TLBCM model

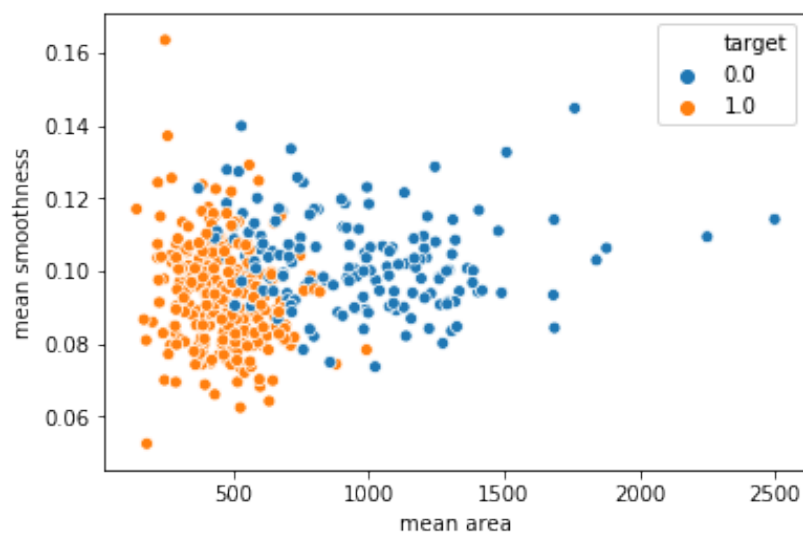


Figure 13. Mean area vs Mean smoothness

233 benign. Figure 9 shows the confusion matrix of the TLBCM model, which evaluates the value predicted
 234 against the target output. 97.2

235 Figure 12 shows loss and accuracy for all iterations of training and testing. The loss value changes
 236 continuously from the beginning of the training to the end. At the end of the training, the value of the loss
 237 is nearly 0.1. The accuracy of the training starts from 70% and reaches the highest of 98.3%.

238 The mean area against the smoothness of the cancer cell can be predicted from Figure ???. The values
 239 produced after the model improvisation. The values correctly predicted in the orange color values as 1
 240 and the wrongly predicted data was indicated as 0 in the blue color.

241 The figure 13 shows the mean area against the smoothness of the cancer cell. The values produced
 242 after the model improvisation. The values correctly predicted in the orange color values as 1 and the
 243 wrongly predicted data was indicated as 0 in the blue color.

244 **Comparative Analysis**

245 The proposed model is compared with other recent models implemented by other researchers. Compared
 246 to the other studies, two types of datasets are used instead of focusing on one dataset, which increases the
 247 learning capacity of the model. The additional added advantage of the proposed work is the pre-trained
 248 classifier. In addition, the model has a fully connected layer that could be integrated into the pre-trained

| Model | Accuracy | Precision | Recall | F1 score |
|---------------|----------|-----------|--------|----------|
| TLBCM | 98.3% | 0.65 | 0.95 | 0.77 |
| CNN+LSTM | 82.5% | 0.62 | 0.85 | 0.70 |
| ResNet + LSTM | 90.1% | 0.59 | 0.92 | 0.75 |
| SVM | 87% | 0.95 | 0.95 | 0.95 |
| Decision Tree | 82% | 0.90 | 0.90 | 0.91 |

Table 5. Proposed Model Comparison with previous research methods

249 model as a Convolution Neural Network (CNN).

250 The table 5 Shows the accuracy value of the proposed model against the previous models. The model
251 CNN+LSTM achieves only 82.5

252 CONCLUSION AND DISCUSSION

253 Many researchers use the machine learning algorithms KNN, SVM, and Decision trees to detect breast
254 cancer from different data sets. This image feature data is monitored continuously using CPS in the
255 network. Although these methods perform well, the handcrafted extracted features make the model
256 complex, and cancer detection is also delayed. This paper proposes the method TLBCM, which combines
257 Resnet, Dense net, and CNN network to effectively classify breast cancer to predict whether it is malignant
258 or benign. The Resnet and Densenet are used as transfer learning for identifying the dataset's features.
259 The experiment has demonstrated the benefits of transfer learning for the job of interest, even when
260 it is between unrelated tasks. To begin the learning process, pre-trained weights should be used as
261 initialization. The loaded weights must then be gradually fine-tuned to train the new datasets to the
262 network. Backpropagation on the layers with a low learning rate is resumed to accomplish this. The
263 experimental results show that TLBCM with CPS performs better than the existing method. The dataset
264 Breast Cancer Wisconsin (Diagnostic) and Breast Cancer Histopathological Database (BreakHis) are
265 used in the proposed paper. The proposed work has achieved 98.3Several tips are offered to improve the
266 creation and training of a neural network model based on the proposed experiments. It is demonstrated
267 that neural networks outperform state-of-the-art techniques for huge training set sizes. Similarly, it is
268 shown that transfer learning is feasible for a short training set and significantly enhances the model's
269 performance. The effects of the critical hyper-parameters are assessed, and the performance of neural
270 networks against the current best practices is also evaluated. Additionally, transfer learning strategies'
271 efficacy is examined in various experimental configurations. The security of the health or patient health
272 data is protected sensitively using CPS. It results in approaching the earlier therapy and reducing the death
273 rate of women due to breast cancer. Future work can be extended to localize the breast tissues with many
274 datasets. Future studies will concentrate on finding the strategies to use the unique characteristics of the
275 multi-labeled problem to develop a joint image-label embedding that characterizes both the semantics
276 label dependency and the relevance of the image-label relationship. To construct an effective, reliable,
277 and potent computer-aided diagnosis system for early breast cancer diagnosis, it is also better to include
278 imaging modalities other than mammography in the learning process. As a result, it will benefit from
279 additional rich representations that already exist.

280 CONFLICT OF INTEREST

281 There are no competing interests were present.

282 ACKNOWLEDGEMENT

283 The study was supported by the SPEV project, run by the faculty of informatics and management, at the
284 University of Hradec Kralove, Czech Republic.

285 REFERENCES

- 286 [1] Alkhaleefah, M., Ma, S.-C., Chang, Y.-L., Huang, B., Chittam, P. K., and Achhannagari, V. P. (2020).
287 Double-shot transfer learning for breast cancer classification from x-ray images. *Applied Sciences*,
288 10(11):3999.

- 289 [2] Andreadis, I. I., Spyrou, G. M., and Nikita, K. S. (2014). scheme for mammography empowered with
290 topological information from clustered microcalcifications' atlases. *IEEE Journal of Biomedical and*
291 *Health Informatics*, 19(1):166–173.
- 292 [3] Bengio, Y., Courville, A., and Vincent, P. (2013). Representation learning: A review and new
293 perspectives. *IEEE transactions on pattern analysis and machine intelligence*, 35(8):1798–1828.
- 294 [4] Chen, T. and Chefd'Hotel, C. (2014). Deep learning based automatic immune cell detection for
295 immunohistochemistry images. In *International workshop on machine learning in medical imaging*,
296 pages 17–24. Springer.
- 297 [5] Ciresan, D., Giusti, A., Gambardella, L., and Schmidhuber, J. (2012). Deep neural networks segment
298 neuronal membranes in electron microscopy images. *Advances in neural information processing*
299 *systems*, 25.
- 300 [6] Cruz-Roa, A., Basavanthally, A., González, F., Gilmore, H., Feldman, M., Ganesan, S., Shih, N.,
301 Tomaszewski, J., and Madabhushi, A. (2014). Automatic detection of invasive ductal carcinoma in
302 whole slide images with convolutional neural networks. In *Medical Imaging 2014: Digital Pathology*,
303 volume 9041, page 904103. SPIE.
- 304 [7] Cruz-Roa, A. A., Arevalo Ovalle, J. E., Madabhushi, A., and González Osorio, F. A. (2013). A
305 deep learning architecture for image representation, visual interpretability and automated basal-cell
306 carcinoma cancer detection. In *International conference on medical image computing and computer-*
307 *assisted intervention*, pages 403–410. Springer.
- 308 [8] Dhungel, N., Carneiro, G., and Bradley, A. P. (2015). Deep learning and structured prediction for the
309 segmentation of mass in mammograms. In *International Conference on Medical image computing and*
310 *computer-assisted intervention*, pages 605–612. Springer.
- 311 [9] Ekici, S. and Jawzal, H. (2020). Breast cancer diagnosis using thermography and convolutional neural
312 networks. *Medical hypotheses*, 137:109542.
- 313 [10] ElOuassif, B., Idri, A., Hosni, M., and Abran, A. (2021). Classification techniques in breast
314 cancer diagnosis: a systematic literature review. *Computer Methods in Biomechanics and Biomedical*
315 *Engineering: Imaging & Visualization*, 9(1):50–77.
- 316 [11] Esteva, A., Kuprel, B., and Thrun, S. (2015). Deep networks for early stage skin disease and skin
317 cancer classification. project report.
- 318 [12] Ganesan, K., Acharya, U. R., Chua, C. K., Min, L. C., Abraham, K. T., and Ng, K.-H. (2012).
319 Computer-aided breast cancer detection using mammograms: a review. *IEEE Reviews in biomedical*
320 *engineering*, 6:77–98.
- 321 [13] Hussain, Z., Gimenez, F., Yi, D., and Rubin, D. (2017). Differential data augmentation techniques
322 for medical imaging classification tasks. In *AMIA annual symposium proceedings*, volume 2017, page
323 979. American Medical Informatics Association.
- 324 [14] Jamieson, A. R., Drukker, K., and Giger, M. L. (2012). Breast image feature learning with adaptive
325 deconvolutional networks. In *Medical Imaging 2012: Computer-Aided Diagnosis*, volume 8315, pages
326 64–76. SPIE.
- 327 [15] Karahaliou, A. N., Boniatis, I. S., Skiadopoulou, S. G., Sakellaropoulos, F. N., Arikidis, N. S., Likaki,
328 E. A., Panayiotakis, G. S., and Costaridou, L. I. (2008). Breast cancer diagnosis: analyzing texture of
329 tissue surrounding microcalcifications. *IEEE transactions on information technology in biomedicine*,
330 12(6):731–738.
- 331 [16] Kaur, P., Singh, G., and Kaur, P. (2019). Intellectual detection and validation of automated mam-
332 mogram breast cancer images by multi-class svm using deep learning classification. *Informatics in*
333 *Medicine Unlocked*, 16:100151.
- 334 [17] Khan, S., Hussain, M., Aboalsamh, H., and Bebis, G. (2017). A comparison of different gabor feature
335 extraction approaches for mass classification in mammography. *Multimedia Tools and Applications*,
336 76(1):33–57.
- 337 [18] Kwon, A., Chae, I. H., You, E., Kim, S. H., Ahn, S.-y., Lee, O.-J., Park, Z.-Y., Rhee, S., Huh,
338 Y. H., and Song, W. K. (2020). Extra domain a-containing fibronectin expression in spin90-deficient
339 fibroblasts mediates cancer-stroma interaction and promotes breast cancer progression. *Journal of*
340 *Cellular Physiology*, 235(5):4494–4507.
- 341 [19] LeCun, Y., Bengio, Y., Hinton, G., et al. (2015). Deep learning. *nature*, 521 (7553), 436-444. *Google*
342 *Scholar Google Scholar Cross Ref Cross Ref*.
- 343 [20] LeCun, Y., Kavukcuoglu, K., and Farabet, C. (2010). Convolutional networks and applications in

- 344 vision. In *Proceedings of 2010 IEEE international symposium on circuits and systems*, pages 253–256.
345 IEEE.
- 346 [21] Li, H., Meng, X., Wang, T., Tang, Y., and Yin, Y. (2017). Breast masses in mammography classifica-
347 tion with local contour features. *Biomedical engineering online*, 16(1):1–12.
- 348 [22] Litjens, G., Kooi, T., Bejnordi, B. E., Setio, A. A. A., Ciampi, F., Ghafoorian, M., Van Der Laak,
349 J. A., Van Ginneken, B., and Sánchez, C. I. (2017). A survey on deep learning in medical image
350 analysis. *Medical image analysis*, 42:60–88.
- 351 [23] Lo, S.-C. B., Chan, H.-P., Lin, J.-S., Li, H., Freedman, M. T., and Mun, S. K. (1995). Artificial
352 convolution neural network for medical image pattern recognition. *Neural networks*, 8(7-8):1201–1214.
- 353 [24] Maheswaran, S., Sathesh, S., Gayathri, M., Bhaarathei, E., and Kavin, D. (2020a). Design and devel-
354 opment of chemical free green embedded weeder for row based crops. *Journal of Green Engineering*,
355 10(5):2103–2120.
- 356 [25] Maheswaran, S., Sathesh, S., Priyadarshini, P., and Vivek, B. (2017). Identification of artificially
357 ripened fruits using smart phones. In *2017 international conference on intelligent computing and
358 control (I2C2)*, pages 1–6. IEEE.
- 359 [26] Maheswaran, S., Vivek, B., Sivaranjani, P., Sathesh, S., and Pon Vignesh, K. (2020b). Development of
360 machine learning based grain classification and sorting with machine vision approach for eco-friendly
361 environment. *Journal of Green Engineering*, 10(3):526–543.
- 362 [27] Mahroogh, M., Ashraf, A. B., Daye, D., McDonald, E. S., Rosen, M., Mies, C., Feldman, M., and
363 Kontos, D. (2015). Pharmacokinetic tumor heterogeneity as a prognostic biomarker for classifying
364 breast cancer recurrence risk. *IEEE Transactions on Biomedical Engineering*, 62(6):1585–1594.
- 365 [28] Malon, C. D. and Cosatto, E. (2013). Classification of mitotic figures with convolutional neural
366 networks and seeded blob features. *Journal of pathology informatics*, 4(1):9.
- 367 [29] Nassif, A. B., Talib, M. A., Nasir, Q., Afadar, Y., and Elgendy, O. (2022). Breast cancer detection
368 using artificial intelligence techniques: A systematic literature review. *Artificial Intelligence in
369 Medicine*, page 102276.
- 370 [30] Oyelade, O. N. and Ezugwu, A. E.-S. (2020). A state-of-the-art survey on deep learning methods for
371 detection of architectural distortion from digital mammography. *IEEE Access*, 8:148644–148676.
- 372 [31] Perre, A. C., Alexandre, L. A., and Freire, L. C. (2018). Lesion classification in mammograms
373 using convolutional neural networks and transfer learning. *Computer Methods in Biomechanics and
374 Biomedical Engineering: Imaging & Visualization*.
- 375 [PUB et al.] PUB, M. H., Bowyer, K., Kopans, D., Moore, R., and Kegelmeyer, P. The digital database for
376 screening mammography. In *Proceedings of the Fifth International Workshop on Digital Mammography*,
377 pages 212–218.
- 378 [33] Rao, V. M., Levin, D. C., Parker, L., Cavanaugh, B., Frangos, A. J., and Sunshine, J. H. (2010). How
379 widely is computer-aided detection used in screening and diagnostic mammography? *Journal of the
380 American College of Radiology*, 7(10):802–805.
- 381 [34] Shen, D., Wu, G., and Suk, H.-I. (2017). Deep learning in medical image analysis. *Annual review of
382 biomedical engineering*, 19:221.
- 383 [35] Shu, X., Zhang, L., Wang, Z., Lv, Q., and Yi, Z. (2020). Deep neural networks with region-based
384 pooling structures for mammographic image classification. *IEEE transactions on medical imaging*,
385 39(6):2246–2255.
- 386 [36] Spanhol, F. A., Oliveira, L. S., Petitjean, C., and Heutte, L. (2015). A dataset for breast cancer
387 histopathological image classification. *Ieee transactions on biomedical engineering*, 63(7):1455–1462.
- 388 [37] Sun, D., Wang, M., Feng, H., and Li, A. (2017). Prognosis prediction of human breast cancer
389 by integrating deep neural network and support vector machine: supervised feature extraction and
390 classification for breast cancer prognosis prediction. In *2017 10th International Congress on Image
391 and Signal Processing, BioMedical Engineering and Informatics (CISP-BMEI)*, pages 1–5. IEEE.
- 392 [38] Wang, Z., Zhang, L., Shu, X., Lv, Q., and Yi, Z. (2020). An end-to-end mammogram diagnosis:
393 A new multi-instance and multiscale method based on single-image feature. *IEEE Transactions on
394 Cognitive and Developmental Systems*, 13(3):535–545.
- 395 [39] Zhang, Y.-D., Wang, S.-H., Liu, G., and Yang, J. (2016). Computer-aided diagnosis of abnormal
396 breasts in mammogram images by weighted-type fractional fourier transform. *Advances in Mechanical
397 Engineering*, 8(2):1687814016634243.